HHS Public Access

Author manuscript

ACS Biomater Sci Eng. Author manuscript; available in PMC 2021 March 25.

Published in final edited form as:

ACS Biomater Sci Eng. 2019 December 09; 5(12): 6395–6404. doi:10.1021/acsbiomaterials.9b01205.

Microporous Bio-orthogonally Annealed Particle Hydrogels for Tissue Engineering and Regenerative Medicine

Alisa Isaac[1,‡], **Faraz Jivan**[1,‡], **Shangjing Xin**[1], **Jacob Hardin**[1], **Xianghong Luan**[2], **Mirali Pandya**[2], **Thomas G. H. Diekwisch**[2], **Daniel L. Alge**[1,3,*]

[1]Department of Biomedical Engineering, Texas A&M University, College Station, TX, USA 77843

[2]Department of Periodontics, Texas A&M University, Dallas, TX, USA 75246

[3]Department of Materials Science and Engineering, Texas A&M University, College Station, TX, USA 77843

Abstract

Microporous annealed particle (MAP) hydrogels are an emerging class of biomaterials with the potential to improve outcomes in tissue repair and regeneration. Here, a new MAP hydrogel platform comprising poly(ethylene) glycol (PEG) hydrogel microparticles that are annealed *in situ* using bio-orthogonal tetrazine click chemistry is reported (*i.e.*, TzMAP hydrogels). Briefly, clickable PEG-peptide hydrogel microparticles with extracellular matrix mimetic peptides to permit cell adhesion and enzymatic degradation were fabricated via submerged electrospraying and stoichiometrically controlled thiol-norbornene click chemistry. Subsequently, unreacted norbornene groups in the microparticles were leveraged for functionalization with bioactive proteins as well as annealing into TzMAP hydrogels via the tetrazine-norbornene click reaction, which is highly selective and proceeds spontaneously without requiring an initiator or catalyst. The results demonstrate that the clickable particles can be easily applied to a tissue-like defect and then annealed into an inherently microporous structure *in situ*. In addition, the ability to produce TzMAP hydrogels with heterogeneous properties by incorporating multiple types of hydrogel microspheres is demonstrated, first with fluorophore-functionalized hydrogel microparticles and then with protein-functionalized hydrogel microparticles. For the latter, tetrazine-modified alkaline phosphatase was conjugated to PEG hydrogel microparticles, which were mixed with non-functionalized microparticles and used to produce TzMAP hydrogels. A biomimetic mineralized/non-mineralized interface was then produced upon incubation in calcium glycerophosphate. Finally, platelet-derived growth factor–BB (PDGF-BB) and human periodontal ligament stem cells (PDLSC) were incorporated into the TzMAP hydrogels during the annealing step to demonstrate their potential for delivering regenerative therapeutics, specifically for periodontal tissue regeneration. *In vitro* characterization revealed excellent PDGF-BB retention as well as PDLSC growth and spreading. Moreover, PDGF-BB loading increased PDLSC proliferation within hydrogels by 90% and more than doubled the average volume per cell. Overall, these results

*Corresponding author: Tel.: 979-458-9248, Fax: 979-845-4450; dalge@tamu.edu.

‡A.I. and F.J. contributed equally to this work.

SUPPORTING INFORMATION

PDGF-BB modified ELISA data, representative live/dead staining images.

demonstrate that TzMAP hydrogels are a versatile new platform for the delivery of stem cells and regenerative factors.

Graphical Abstract

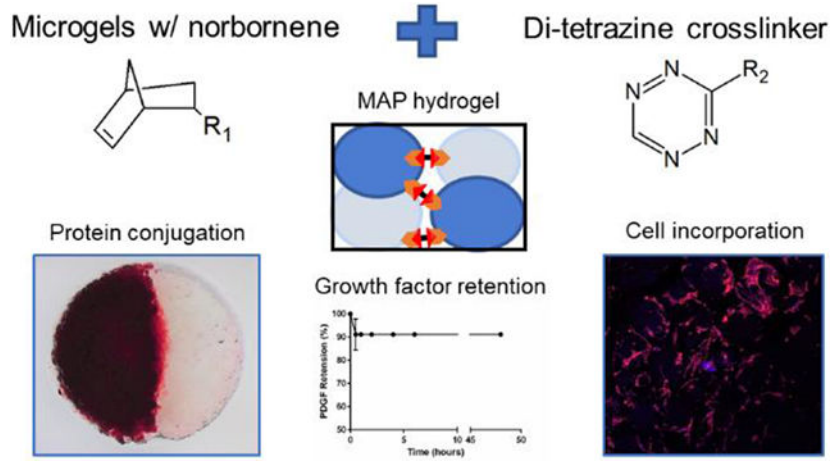

Keywords

hydrogel; click chemistry; bioconjugation; microparticle; periodontal

INTRODUCTION

Hydrogels are among the most popular materials used in tissue engineering and regenerative medicine and have a long track record of use for delivering growth factors and cells [1, 2]. Microporous annealed particle (MAP) hydrogels, which are fabricated from spherical hydrogel microparticles that are linked together, are a relatively new class of hydrogels that is attracting growing interest. A key advantage of MAP hydrogels is that their microporosity and pore interconnectivity allow cells to spread and proliferate better compared to conventional nanoporous hydrogels, which has been shown to accelerate tissue healing and regeneration *in vivo* compared to conventional hydrogels [3, 4]. In addition, cells interact with the microgel surfaces rather than being embedded within a nanoporous polymer network, providing an opportunity to direct cellular responses by engineering the physicochemical properties of microgels based on the well-established knowledge of 2D cell-material interactions [5]. MAP hydrogels can also be constructed from multiple types of microgels with different physicochemical properties, which is another important advantage compared to conventional hydrogels that could be exploited to create biomaterials with controlled heterogeneity. Additionally, MAP hydrogels can be 3D printed, as we recently demonstrated [6].

A variety of synthetic strategies can be used to anneal hydrogel microparticles into MAP hydrogels. The seminal work of Griffin *et al.* laid the foundation for annealing microparticles by chemically linking complementary functional groups, which in their study were lysine and glutamine residues linked together via transglutaminase [3]. That strategy has

continued to be used [4, 7], but alternative non-enzymatic annealing chemistries have also been reported such as vinyl polymerizations, strain-promoted azide-alkyne cycloadditions [8-10], and adamantane-cyclodextrin guest-host interactions [10]. In addition, we recently reported the use of thiol-norbornene click photopolymerization. In our work, we produced poly(ethylene glycol) (PEG) hydrogel microparticles via submerged electrospraying and thiol-norbornene step-growth photopolymerization, which allowed us to tune the physicochemical properties of the microparticles to influence how cells responded to the materials [11]. We also controlled the stoichiometry so that the microparticles contained an excess of norbornene groups. This design enabled facile annealing with a PEG-di-thiol linker and a secondary thiol-norbornene reaction. While this approach was effective, the requirement to photoinitiate the annealing reaction could be a barrier to clinical adoption. Thus, we sought to develop an alternative chemical strategy for annealing that would be compatible with our method of producing PEG hydrogel microparticles.

Tetrazine click chemistry is an ideal approach to annealing norbornene-containing hydrogel microspheres into MAP hydrogels. In general, tetrazine click chemistry refers to the inverse-electron demand Diels-Alder reaction between *s*-tetrazines and electron-rich dienophiles, such as norbornene and trans-cyclooctene [12]. Tetrazine click reactions are generally fast, efficient, selective, proceed under mild conditions, and produce only nitrogen gas, which is an inoffensive byproduct. Moreover, tetrazine click reactions proceed readily under physiologic conditions, do not require the addition of an initiator or catalyst, and can be performed in the presence of living cells and even within living animals [12]. Thus, tetrazine click chemistry is regarded as bio-orthogonal, which is a key advantage. Importantly, the tetrazine-norbornene reaction has been used as a primary crosslinking chemistry in several studies on hydrogel biomaterials in recent years [13-15]. We also recently reported on the use of sequential thiol-norbornene and tetrazine-norbornene click reactions to synthesize norbornene-containing PEG hydrogel microparticles and then functionalize them with bioactive proteins, namely alkaline phosphatase (ALP) and glucose oxidase [16]. Based on this prior work, we hypothesized that a di-tetrazine linker could be used analogously to PEG-di-thiol in our previous work to anneal PEG hydrogel microparticles into MAP hydrogels (*i.e.*, TzMAP hydrogels).

The objective of this study was to test our hypothesis and demonstrate the potential of TzMAP hydrogels for the development of tissue regeneration therapies. First, we verified MAP hydrogel formation and tested if TzMAP hydrogels could be produced within a tissue-like defect. Subsequently, since the potential to use multiple types of hydrogel microparticles is an important feature of MAP hydrogels, we investigated the potential to produce heterogenous and spatially patterned TzMAP hydrogels. We did this first using fluorophore-labelled microparticles and subsequently using microparticles that were functionalized with ALP using tetrazine click chemistry, as in our prior work, to selectively mineralize a region of the material. Finally, to demonstrate suitability of TzMAP hydrogels to deliver regenerative therapeutics, we examined PDGF-BB and PDLSC incorporation during annealing.

EXPERIMENTAL METHODS

Materials

PEG-tetra-norbornene (PEG-NB) was synthesized via esterification of PEG-tetra-OH (5 kDa; JenKem USA) with 5-norbornene-2-carboxylic acid (Sigma Aldrich), as previously described [17]. PEG-di-tetrazine was synthesized by functionalizing a PEG-di-amine (3.4 kDa; Laysan Bio) with 5-(4-(1,2,4,5-tetrazin-3-yl)-benzylamino)-5-oxopentanoic acid, synthesized as previously described [13]. Lithium acylphosphinate photoinitiator (LAP) was synthesized as previously described [18]. End-group functionalization of PEG-NB and PEG-di-tetrazine, and LAP structure were confirmed by ^{1}H NMR. Cell adhesive peptide CGRGDS was synthesized with standard solid-phase Fmoc synthesis methods on Rink amide resin (Novabiochem). The peptide was purified by high pressure liquid chromatography (ThermoFisher Dionex UltiMate 3000) using water and acetonitrile with 0.1% trifluoroacetic acid as the mobile phase and C18 column as the stationary phase. The composition of the peptide was verified by matrix assisted laser desorption-ionization time-of-flight mass spectroscopy (MALDI-TOF MS; $[M+H]_{theoretical}$ = 593.6, $[M+H]_{observed}$ = 593.5). Matrix metalloproteinase (MMP) degradable crosslinker KCGPQGIWGQCK was purchased from BL Biochem. Lyophilized peptides were reconstituted in phosphate buffered saline (PBS; pH = 7.4). Concentration of peptides was determined by measuring absorbance at 205 nm via spectrophotometer [19].

PEG hydrogel microparticle synthesis

PEG microgels were fabricated via submerged electrospraying, as previously described [6, 11]. Briefly, PEG-NB (5 kDa, 10 wt%), MMP-degradable crosslinker (KCGPQGIWGQCK, 0.75:1 thiol-ene molar ratio), cell-adhesive peptide (CGRGDS, 1 mM) and lithium acylphosphinate photoinitiator (LAP, 10 mM) were dissolved in PBS. Pre-polymer solution was electrosprayed (12 mL/hr, 4.0 kV, 22-gauge needle, 16 mm tip to ring distance) into light mineral oil (Fisher Scientific) with Span-80 (0.05 wt%) and photopolymerized with 365 nm light at 60 mW/cm^2. Microgels were isolated and washed twice with PBS via centrifugation (4500 rpm, 15 min) followed by a sterilization wash in 70% ethanol, and then two washes in sterile PBS.

TzMAP hydrogel formation and characterization

PEG hydrogel microparticles were packed into a 6-mm diameter silicone mold (50 μL volume, 14.7 mM free norbornene on microparticles). PEG-di-Tz crosslinker was added (2 mM, 12 μL) and allowed to anneal microparticles for 1 hour at 37 °C [13]. To verify annealing, the storage moduli of uncrosslinked and tetrazine crosslinked microgels were measured using rheology. Crosslinked and uncrosslinked microgels were placed under an 8-mm parallel plate tool (TA Instruments, Discovery DH-2) and an oscillatory time sweep (1% strain, 1 rad/sec angular freq.) was performed to obtain the shear storage modulus (G'; n = 3). In addition, to verify microporosity, TzMAP hydrogels were soaked in a 5 mg/mL solution of high molecular weight tetramethylrhodamine isothiocyanate-labeled dextran (155 kDa, Sigma) and imaged using confocal fluorescence microscopy (Olympus FV1000). Z-stack images were taken (200 um depth, 4.46 um step size) and porosity was determined via FIJI software by thresholding images to black & white and using the "Voxel Counter" plugin

to measure the volume of pore space (white voxels) and the total stack volume (total voxels). The following formula was used to calculate the percent microporosity:

$$\text{Porosity}\,(\%) = (\text{white voxels}) \,/\, (\text{total voxels}) \times 100\,\%$$

In situ TzMAP hydrogel annealing in a tissue-like defect

To demonstrate *in situ* TzMAP hydrogel assembly, a tissue-like defect was made at the edge of a plaster block using a small end-mill bit. A glass slide was taped over the edge to provide containment for the microgels/crosslinker solution as well as provide cross-sectional visibility. Images were taken with a Canon DSLR camera at each step during the TzMAP hydrogel fabrication process (*i.e.*, packing of microgels, addition of crosslinker solution, etc.). Alexa-548 functionalized microgels were utilized as they were colored blue under ambient lighting conditions, allowing for easy visibility of the microgels. After TzMAP hydrogel crosslinking, the wedge-shaped hydrogel was removed to verify annealing.

Stereomicroscopy imaging

Annealed constructs (6-mm diameter) were imaged under brightfield using a Zeiss SteREO Discovery microscope to show a generic TzMAP hydrogel. To enable fluorescence visualization, electrosprayed microgels were functionalized by incubation with Alexa-488 NHS Ester or Alexa-548 NHS Ester for 1 hour at room temperature, resulting in fluorophore conjugation to the peptides in the microgels. Differentially colored microgels were then combined and added to an 8-mm diameter cylindrical silicone mold to make a heterogenous TzMAP hydrogel with various patterns (half & half and uniformly mixed). They were imaged using the Zeiss SteREO microscope in brightfield and using the green fluorescence filter.

Protein conjugation to TzMAP hydrogels

Texas Red-labelled Ovalbumin.—Texas Red-labelled Ovalbumin (1.5 mg/mL, Life Technologies) was reacted with 5-(4-(1,2,4,5-tetrazin-3-yl)-benzylamino)-5-oxopentanoic acid N-hydroxy succinimidyl ester (Tz-NHS, 10 molar equivalents, Sigma Aldrich), Tz-NHS with a 5 unit PEG spacer (Tz-PEG-NHS, 10 molar equivalents, Click Chemistry Tools) or with dimethyl sulfoxide (non-functionalized protein, NF-Ovalbumin) for 1 hour at room temperature. Tetrazine-functionalized and non-functionalized fluorescent ovalbumin (1 mg/mL) was reacted with norbornene-containing PEG microgels (50 μL) for 1 hour at room temperature, after which the microgels were washed four times with PBS and then annealed with PEG-di-tetrazine (2 mM) for 1 hour at room temperature to form TzMAP hydrogels. The TzMAP hydrogels were then imaged via confocal fluorescence microscopy and FIJI 3D Viewer plugin was used to generate images and qualitative assess protein conjugation.

Alkaline phosphatase conjugation and characterization.—Tetrazine-functionalized alkaline phosphatase (Tz-ALP) was produced similarly to ovalbumin. Briefly, ALP (25 mg/mL) was incubated with Tz-NHS or Tz-PEG-NHS at three different molar ratios (10x, 20x, and 30x molar equivalents with respect to ALP) for 1 hour at room temperature to yield tetrazine-functionalized ALP (Tz-ALP). Tz-ALP solution was then

incubated with a microgel pellet for 1 hour at 37°C, to allow for the tetrazine-norbornene reaction to conjugate ALP to the microgels, followed by four wash steps with PBS to remove unbound protein.

Protein bioactivity and functionalization of the resulting microgels were characterized via absorbance spectroscopy. ALP activity was assessed using *p*-nitrophenylphosphate (pNPP). 100 μL samples of microgels were placed in a 96-well plate along with 25 μL of pNPP substrate solution (Thermo Fisher). Absorbance values were measured at 405 nm at five-minute intervals for twenty minutes to quantify pNPP conversion. The rate of change was then calculated in order to determine the relative degree of protein activity (n = 3). To quantify ALP loading, the microparticles were degraded with 0.1 M sodium hydroxide overnight and absorbance values were read at 280 nm, leveraging the presence of aromatic rings in the structure of ALP [20]. Protein concentrations were calculated using a standard curve prepared of ALP ranging from 0 to 10 mg/mL (n = 3).

Mineralization of alkaline phosphatase-functionalized TzMAP hydrogels

To demonstrate formation of a mineralized/non-mineralized interface in the TzMAP hydrogels, a batch of ALP-functionalized microgels prepared with 10x Tz-PEG-NHS functionalized ALP were mixed with ALP-free microgels. TzMAP hydrogels were then made in a 6-mm diameter silicone mold as previously described with half of the hydrogel made from ALP-functionalized microgels and the other half with ALP-free microgels. For mineralization, the TzMAP hydrogels were placed in calcium glycerophosphate (0.1 M in ultrapure water) for 1 hour at 37° C, and mineralization was visualized using alizarin red S staining and brightfield imaging on a Zeiss SteREO Discovery microscope. Higher magnification images were also taken using brightfield imaging on a Zeiss AxioVert.A1 microscope.

PDGF-BB Loading and Retention

TzMAP hydrogels were prepared as previously described. For PDGF-BB retention studies, 120 ng of human recombinant PDGF-BB (Peprotech) was added during the microgel annealing step. TzMAP hydrogels were incubated at 37 °C in 1 mL PBS. At predetermined time points, 1 mL of PBS was removed for analysis on a PDGF-BB ELISA (Peprotech), and 1 mL of fresh PBS was replaced. The concentration of PDGF-BB released was determined by comparing the absorbance values of the samples to the standard curve provided in the kit. PDGF-BB retention was calculated by subtracting measured release values from the loaded PDGF-BB amount. (n = 3).

Additionally, PDGF-BB loaded MAP hydrogels were tested directly using a modified ELISA to monitor growth factor retention. Again, 120 ng of PDGF-BB was loaded within TzMAP hydrogels that were annealed as described above. TzMAP hydrogels were immediately tested after annealing or after 48 hrs incubation in PBS at 37 °C. In brief, TzMAP hydrogels were transferred into a 96-well plate, blocked in 1% BSA for 1 hour, incubated with PDGF-BB detection antibody (0.25 μg/mL) for 2 hours, followed by Avidin-HRP conjugate (1:2000) for 30 minutes. TMB liquid substrate (100 μL) was added and allowed to develop for 4 minutes before stopping with TMB stop solution (100 μL, 1%

HCl). Solution was moved to a new well and read *via* an absorbance plate reader (450 nm). Absorbance values were normalized to a blank MAP hydrogel (n = 3).

PDLSC incorporation and effects of PDGF-BB loading

PDLSCs were isolated and expanded as previously described [21]. Briefly, periodontal ligament was scraped off of dissected 3rd molars' roots and digested in collagenase/dispase. Use of human third molars was approved by University of Illinois at Chicago Office for the Protection of Research Subjects. Primary cells were plated and cultured in Dulbecco's modified eagle's medium (DMEM), and plastic adherent cells were passaged once they reached confluency. After 3 passages, the cells were expanded and treated with recombinant human fibroblast growth factor (rhFGF) for 2 weeks or fibroblast growth factor 2 (FGF2) and connective tissue growth factor (CTGF) for 10 days. PDLSCs were then transferred to growth medium (high glucose DMEM supplemented with 10% FBS and 1% P/S) until use. PDLSCs were kept at 10 passages or lower for all experiments.

TzMAP hydrogels were prepared as described above. 50,000 PDLSCs and 120 ng of recombinant human PDGF-BB (Peprotech) were incorporated during the microgel annealing step for each 50 μL hydrogel. Constructs were incubated in 1 mL of growth medium at 37 °C, 5% CO_2 for 5 days. Media was changed every 2 days. PDLSCs in TzMAP hydrogels without PDGF-BB were used as a negative control (n = 6).

PDLSC viability

PDLSCs were incorporated in TzMAP hydrogels during annealing as described above. After 24 hours, cells were stained with calcein-AM (Marker Gene Technologies, 1:2000, 2 μM) and ethidium homodimer (Chemodex, 1:500, 4 μM) for 30 minutes at room temperature and imaged on a Zeiss AxioVert.A1 microscope to determine the percentage of live cells (n = 3).

PDLSC spreading and proliferation

After 5 days, TzMAP hydrogels containing PDLSCs were fixed with 4% formaldehyde for 15 minutes at 4 °C, followed by PBS washing. The cells were then stained with Rhodamine Phalloidin (Molecular Probes) for 1 hour at room temperature, washed with PBS to remove excess staining solution, and finally stained with DAPI (Cayman Chemical) for 15 minutes at room temperature. Cell-laden constructs were imaged (200 μm z-stacks) using confocal fluorescence microscopy (Olympus FV1000). Cell nuclei were counted from the z-stack images using the "Particle Counter" plugin in FIJI to quantify cell number, and cell area was quantified using the "Voxel Counter" plugin in FIJI to determine cell spreading.

Statistical Analysis

Statistical analysis of the quantitative data was performed using GraphPad prism. Statistical significance of ALP loading and activity were determined by two-way ANOVA with post-hoc comparisons, and statistical significance of storage modulus, cell number and volume, and modified PDGF-BB ELISA were determined by two-tailed Student's t-test ($p < 0.05$).

RESULTS

TzMAP hydrogel formation

Submerged electrospraying produced PEG hydrogel microparticles that were approximately 150 μm in diameter and contained unreacted norbornene groups for annealing. The synthesis of the hydrogel microparticles was similar to our previous work, in which we showed via ^{1}H NMR that stoichiometric control over the thiol-ene reaction can be leveraged to produce microparticles with free norbornene groups that can subsequently be utilized for tetrazine click reactions [16]. The hydrogel microparticles were also crosslinked with a well-known MMP cleavable peptide sequence[13,17] to make them susceptible to cell-mediated degradation, since degradability is critical for use in tissue engineering. For clinical application, we envision the microparticles being applied directly to a tissue defect either via syringe or by being manually scooped/packed-in and then crosslinked *in situ*. We are particularly interested in periodontal defects, with the TzMAP hydrogels being used to deliver therapeutics like PDGF-BB and PDLSCs (Figure 1). To demonstrate the utility of our TzMAP hydrogels for this application and simulate a periodontal defect, microgels were packed into a wedge-shaped mold and crosslinked with the addition of PEG-di-tetrazine (Figure 2a-c). The resulting 3D hydrogel after annealing was well-packed, cohesive, and perfectly matched the wedge defect (Figure 2d).

The TzMAP hydrogels were further characterized by microscopy and rheology. Stereomicroscopy revealed a bumpy surface topography, and individual microparticles could be visualized (Figure 2e). Shear rheological tests showed a statistically significant 1.7-fold increase in storage modulus from 1.16 kPa to 1.97 kPa after annealing with the PEG-di-tetrazine (Figure 2f), indicating tetrazine crosslinking enhanced mechanical properties. To visualize pore size within the TzMAP hydrogels, the microgels were perfused with tetramethylrhodamine isothiocyanate-labelled dextran and imaged via confocal microscopy. Imaging demonstrated the presence of substantial void space and interconnected pores. The average porosity was measured to be 26.0 ± 9.1 %, with pore sizes ranging from tens to hundreds of microns (Figure 2g).

Heterogeneous TzMAP hydrogels were produced using fluorophore-labelled microgels. Incubation of microgels with Alexa-488 and Alexa-546 NHS esters resulted in distinct color and fluorescence properties due to fluorophore conjugation to amine groups in the peptides. These colored microgels were easily distinguished from one another in TzMAP hydrogels when uniformly mixed and when a half/half pattern was produced. In the bright-field images, Alexa-488-labelled microgels in the TzMAP hydrogel appeared yellow whereas Alexa-546-labelled ones appeared blue (Figure 3a,b). Alexa-488-labelled microgels also fluoresced brightly in green-channel fluorescence images, whereas the Alexa-546-labelled ones appeared dark (Figure 3c,d).

Protein-functionalized TzMAP hydrogels

Unreacted norbornene groups in the microgels were successfully leveraged for protein functionalization prior to annealing using the same tetrazine click reaction. Texas Red-labelled Ovalbumin was reacted with Tz-NHS or Tz-PEG-NHS to form fluorescent

tetrazine-modified protein. Non-functionalized protein was used as a control. Subsequently, the protein was incubated with microgels, which were then annealed into TzMAP hydrogels. Images obtained from confocal microscopy revealed qualitatively that TzMAP hydrogels produced from Tz-NHS and Tz-PEG-NHS showed relatively no difference in fluorescence. While we might expect differences in functionalization based on tetrazine linker structure, some amine groups on ovalbumin have already been used for Texas-Red fluorophore conjugation. Thus, differences between Tz-NHS and Tz-PEG-NHS based on the remaining amine groups available for functionalization may be difficult to observe visually. Regardless, both tetrazine functionalized protein microgels demonstrated significantly more fluorescence than non-functionalized counterparts, indicating the importance of the tetrazine moiety (Figure 4).

After determining successful protein conjugation to TzMAP hydrogels, bioactive protein conjugation was investigated. Tetrazine-functionalized ALP (Tz-ALP) was prepared similarly to ovalbumin with incubation with Tz-NHS and Tz-PEG-NHS, and the tetrazine reagents were tested at 10x, 20x, and 30x equivalents to evaluate this variable. The resulting Tz-ALP or non tetrazine-functionalized ALP (NF-ALP) was reacted with microgels for 1 hour to form ALP-conjugated and ALP-free TzMAP hydrogels, respectively. Interestingly, microgels incubated with Tz-NHS exhibited significantly more protein loading compared to Tz-PEG-NHS across all equivalent groups, and increasing the equivalents of Tz-NHS increased protein loading (Figure 5a). While further investigation is needed to elucidate the reason for the higher loading achieved with Tz-NHS, the bioactivity measurements suggest that increased loading was not necessarily beneficial. Tz-NHS conjugation resulted similar bioactivity compared to Tz-PEG-NHS, and no statistically significant differences in bioactivity were observed between the 10x, 20x, and 30x treatments (Figure 5b).

Finally, based on the bioactivity results, microgels prepared with 10x Tz-PEG-NHS modified ALP were utilized to produce heterogeneous TzMAP hydrogels that were ALP-functionalized on one half and ALP-free on the other. Following incubation with calcium glycerophosphate, these ALP-functionalized TzMAP hydrogels were stained with alizarin red to visualize mineralization. Substantial mineralization was observed only on the ALP-functionalized half of the TzMAP hydrogels and had a distinctive red appearance, while the other half of the hydrogel and control hydrogel (non-protein functionalized) showed no evidence of mineralization (Figure 5c-f).

PDGF-BB and PDLSC incorporation into TzMAP hydrogels

To determine how well the TzMAP hydrogels localize protein for encapsulated cells, 120 ng of PDGF-BB was loaded into 50 μL TzMAP hydrogels during annealing and release was monitored at several time points (30 min, 1 hour, 2 hours, 4 hours, 6 hours, 12 hours, 24 hours, and 48 hours) over a period of 2 days via ELISA. A burst release of approximately 9% of the initial loading concentration of PDGF-BB was observed after 1 hour, and minimal release was observed from 1 hour to 48 hours (Figure 6a). To corroborate this data, PDGF-BB loaded TzMAP hydrogels were also tested via a modified ELISA to directly measure growth factor retained in the hydrogels. Importantly, there was no statistical difference in

growth factor loaded TzMAP hydrogels after 48 hours compared to those at 0 hours (Supporting Information, Figure S1), thereby confirming PDGF-BB retention.

To verify cytocompatibility, PDLSCs were incorporated within TzMAP hydrogels during annleaing and cell viability was measured via live/dead staining. After 24 hours, PDLCs showed good viability (87% ± 5%) within the TzMAP hydrogels (Supporting Information, Figure S2). PDLSCs were then incorporated in PDGF-BB loaded TzMAP hydrogels, fixed, and stained with DAPI and rhodamine phalloidin to examine PDGF-BB retention effects on encapsulated cells. After a 5-day incubation within the TzMAP hydrogels, cell number and cell volume were increased in TzMAP hydrogels with PDGF-BB, shown by increased DAPI and rhodamine phalloidin staining (Figure 6d) compared with PDLSCs in a TzMAP hydrogel with no PDGF-BB. Quantitatively, images obtained from fluorescent confocal microscopy show a significant 89.7% increase in cell count on day 5 in TzMAP hydrogels with PDGF-BB compared to PDGF-BB free controls (Figure 6b). We also evaluated cell spreading by determining total rhodamine phalloidin staining volume per DAPI count to obtain the average volume per cell. Average cell volume increased by 156% on day 5 in TzMAP hydrogels with PDGF-BB compared to the PDGF-BB free controls (Figure 6c).

DISCUSSION

MAP hydrogels are attracting increasing interest in biomaterials research and have shown superior tissue regeneration results compared to conventional nanoporous hydrogels. The work of Griffin et al. examined PEG based MAP hydrogels in a murine skin wound healing model and found that MAP hydrogels increased wound closure, increased cell infiltration within the hydrogel, and had a decreased immune response compared to monolithic hydrogel slabs of the same composition [3]. Also relevant is the work of Nih *et al.* examining hyaluronic acid MAP hydrogels for promoting tissue regeneration following ischemic strokes [4]. In a murine stroke model, the hyaluronic acid-based MAP hydrogels promoted neural progenitor cell migration and led to superior tissue regeneration in comparison to monolithic hyaluronic acid hydrogels. Hou et al. studied gelatin-based MAP hydrogels in an *ex vivo* porcine cornea model and demonstrated increased corneal epithelial cell infiltration in the MAP hydrogel compared to a nonporous gelatin hydrogel [22]. Collectively, these studies show MAP hydrogels' potential for developing improved tissue regeneration strategies.

Here, we report a new MAP hydrogel platform comprising RGD-functionalized, MMP-degradable PEG-based microgels that are prepared via off-stoichiometric thiol-norbornene click chemistry and then annealed with bio-iorthogonal tetrazine click chemistry (*i.e.*, TzMAP hydrogels; Figure 1,2). The use of thiol-norbornene click chemistry, which is photoinitiated and free radical-mediated, permits facile tuning of the physicochemical properties of the microgels [23]. Combining this tunability with the ability to incorporate multiple microgel populations (Figure 3) could be leveraged to develop novel and more effective hydrogels for tissue regeneration. A key feature, however, is the bio-orthogonality of the tetrazine-norbornene click reaction used for annealing. In contrast to our prior work using a secondary thiol-norbornene reaction for annealing, this reaction proceeds readily under mild conditions, without requiring an initiator or catalyst, and can be done in living

systems. It also permits a suitable working time for clinical implementation. We specifically used a hydrogen-terminated tetrazine (Figure 1), which exhibits faster reaction kinetics with norbornene groups compared to methyl-terminated tetrazines [24]. With this chemistry, TzMAP hydrogels become cohesive within minutes after adding a small amount of di-tetrazine crosslinker, which is suitable for injectability.

An additional advantage of our TzMAP hydrogel platform is its compatibility with tetrazine-norbornene click-mediated bioactive protein conjugation (Figure 4). Conjugation to biomaterials can provide sustained but localized presentation of bioactive proteins, which could be broadly useful for tissue engineering. However, mild conjugation chemistries must be used in order to preserve protein bioactivity. Tetrazine click chemistry is a particularly attractive strategy for conjugation, and we previously demonstrated the use of a tetrazine succinimidyl ester (Tz-NHS) for protein functionalization and bio-orthogonal conjugation to PEG microgels [16] and bulk hydrogels [25]. Here, we built on this prior work and compared the effects of two different tetrazines added at varying molar equivalents to ALP. We specifically compared a short tetrazine linker versus a longer tetrazine linker with a flexible PEG chain, which we hypothesized would make the tetrazine moiety more accessible for conjugation to the microgels. However, we found that the shorter tetrazine linker resulted in higher protein conjugation. In addition, while increasing the molar equivalents of tetrazine did increase protein conjugation, this was at the expense of ALP bioactivity (Figure 5). This result in particular is important, as it suggests that the stochastic nature of the succinimidyl ester modification results in a tradeoff between the amount of protein loading achieved and bioactivity preservation, despite the bio-orthogonality of the tetrazine-norbornene click reaction.

Due to its critical role in biomineralization, the ability to conjugate ALP to the microgel building blocks of TzMAP hydrogels presented a unique opportunity to engineer a composite material. To this end, we incubated TzMAP hydrogels that contained ALP-functionalized microgels in one half and ALP-free microgels in the other half with calcium glycerophosphate. Importantly, only the ALP conjugated region of the TzMAP hydrogels produced mineralization, demonstrating not only that the conjugated protein remained bioactive but also that localizing it to a specific region can produce a spatially patterned calcium phosphate-hydrogel composite (Figure 5). These materials could be useful for mimicking complex tissue interfaces such as craniofacial, oral, and musculoskeletal tissues [26, 27]. More complex patterns and multi-phasic materials can also be envisioned and could potentially aid in regenerating multiple tissues types simultaneously, an important challenge in the field of tissue engineering [26]. For example, periodontal tissue healing, which requires the simultaneous regeneration of the periodontal ligament, alveolar bone, and cementum [28], has been especially challenging due to current treatments such as open flap debridement, use of barrier membranes, and use of growth factors having limited regenerative potential [29-35]. Composite TzMAP hydrogels could be promising materials for addressing this challenge.

To evaluate the utility of TzMAP hydrogels for delivering regenerative therapeutics, we incorporated PDGF-BB during annealing. PDGF-BB, which is an isoform of PDGF found in both soft and hard tissues,[36] is of high interest for treating periodontal disease[28]. This chronic inflammatory disease afflicts 47.2% of adults ages 30 and older in the United States

and, if left untreated, will lead to degradation of the periodontal ligament and alveolar bone, speech and masticatory diseases, and premature tooth loss [37, 38]. While PDGF-BB delivery has previously been found to improve periodontal disease outcomes *in vivo* in both canine and non-human primate models [39, 40] and in clinical trials [41], further improvements could potentially be achieved with new delivery systems. Importantly, approximately 91% of the initial loading amount of PDGF-BB was found to be retained within the hydrogel after 48 hours (Figure 6a), suggesting that TzMAP hydrogels can effectively localize this growth factor and serve as a depot of therapeutic protein. While this feature could be leveraged for a cell-free approach to periodontal regeneration, regenerative efficacy could be further augmented by co-delivery of therapeutic cells. In particular, PDLSCs, which can be extracted and isolated from human molars [42], may be needed due to the decreased prevalence of PDLSCs in periodontal disease patients caused from chronic inflammation[43]. Importantly, PDLSCs can be easily incorporated into TzMAP hydrogels during annealing and responded to PDGF-BB loading by significantly increasing their proliferation and spreading (Figure 6b-d). This result confirmed PDGF-BB bioactivity and is in agreement with prior work on the effects of PDGF-BB on PDLSCs *in vitro* [44-47].

CONCLUSIONS

Electrosprayed PEG microgels prepared via off-stoichiometric thiol-norbornene click chemistry were successfully annealed into MAP hydrogels using a PEG-di-tetrazine linker. This approach is amenable to *in situ* MAP hydrogel formation and is expected to be broadly useful for tissue regeneration and repair. One possibility is to combine TzMAP hydrogels with tetrazine click-mediated protein conjugation to engineer functional and even heterogenous materials, as demonstrated with ALP. ALP conjugation was specifically leveraged to produce a mineralized/non-mineralized interface, but recent advances in 3D printing MAP hydrogels could enable the production of more sophisticated heterogenous structures. The mild bio-orthogonal tetrazine click reaction is also attractive for incorporating protein and cellular therapeutics during annealing. TzMAP hydrogels exhibited excellent PDGF-BB retention, and future studies should investigate if other protein therapeutics are similarly retained. PDLSCs were also incorporated into TzMAP hydrogels and increased proliferation and spreading in response to PDGF-BB loaded in the materials, suggesting utility for periodontal regeneration. Future studies should investigate TzMAP hydrogels for this as well as other applications in tissue engineering.

Supplementary Material

Refer to Web version on PubMed Central for supplementary material.

ACKNOWLEDGEMENTS

Research reported in this publication was supported by the National Institute of Arthritis and Musculoskeletal and Skin Diseases of the National Institutes of Health (award number R21AR071625; to D.L.A.), the National Institute of Dental and Craniofacial Research of the National Institutes of Health (award number 5R01DE027930; to T.D.), and a Graduate Research Fellowship from the National Science Foundation (to A.I.).

REFERENCES

1. Lee KY; Mooney DJ, Hydrogels for tissue engineering. Chem Rev 2001, 101 (7), 1869–1880. DOI: 10.1021/cr000108x. [PubMed: 11710233]
2. Nguyen KT; West JL, Photopolymerizable hydrogels for tissue engineering applications. Biomaterials 2002, 23 (22), 4307–4314. DOI:10.1016/s0142-9612(02)00175-8. [PubMed: 12219820]
3. Griffin DR; Weaver WM; Scumpia PO; Di Carlo D; Segura T, Accelerated wound healing by injectable microporous gel scaffolds assembled from annealed building blocks. Nat Mater 2015, 14 (7), 737–44. DOI: 10.1038/nmat4294. [PubMed: 26030305]
4. Nih LR; Sideris E; Carmichael ST; Segura T, Injection of Microporous Annealing Particle (MAP) Hydrogels in the Stroke Cavity Reduces Gliosis and Inflammation and Promotes NPC Migration to the Lesion. Adv Mater 2017, 29 (32). DOI: 10.1002/adma.201606471.
5. Guvendiren M; Burdick JA, Engineering synthetic hydrogel microenvironments to instruct stem cells. Curr Opin Biotechnol 2013, 24 (5), 841–6. DOI:10.1016/j.copbio.2013.03.009. [PubMed: 23545441]
6. Xin S; Chimene D; Garza JE; Gaharwar AK; Alge DL, Clickable PEG hydrogel microspheres as building blocks for 3D bioprinting. Biomater Sci 2019, 7 (3), 1179–1187. DOI:10.1039/C8BM01286E. [PubMed: 30656307]
7. Darling NJ; Sideris E; Hamada N; Carmichael ST; Segura T, Injectable and Spatially Patterned Microporous Annealed Particle (MAP) Hydrogels for Tissue Repair Applications. Advanced Science 2018, 5 (11), 1801046. DOI:10.1002/advs.20180146. [PubMed: 30479933]
8. Sideris E; Griffin DR; Ding Y; Li S; Weaver WM; Di Carlo D; Hsiai T; Segura T, Particle hydrogels based on hyaluronic acid building blocks. ACS Biomater Sci Eng 2016, 2 (11), 2034–2041. DOI:10.1021/acsbiomaterials.6b00444. [PubMed: 33440539]
9. Caldwell AS; Campbell GT; Shekiro KM; Anseth KS, Clickable microgel scaffolds as platforms for 3D cell encapsulation. Adv Healthcare Mater 2017, 6 (15), 1700254. DOI: 10.1002/adhm.201700254.
10. Mealy JE; Chung JJ; Jeong HH; Issadore D; Lee D; Atluri P; Burdick JA, Injectable granular hydrogels with multifunctional properties for biomedical applications. Adv Mater 2018, 30 (20), 1705912. DOI: 10.1002/adma.20170512.
11. Xin S; Wyman OM; Alge DL, Assembly of PEG Microgels into Porous Cell-Instructive 3D Scaffolds via Thiol-Ene Click Chemistry. Adv Healthcare Mater 2018, 7 (11), 1800160. DOI: 10.1002/adhm.201800160.
12. Oliveira B; Guo Z; Bernardes G, Inverse electron demand Diels–Alder reactions in chemical biology. Chem Soc Rev 2017, 46 (16), 4895–4950. DOI:10.1039/c7cs00184c. [PubMed: 28660957]
13. Alge DL; Azagarsamy MA; Donohue DF; Anseth KS, Synthetically tractable click hydrogels for three-dimensional cell culture formed using tetrazine–norbornene chemistry. Biomacromolecules 2013, 14 (4), 949–953. DOI: 10.1021/bm4000508. [PubMed: 23448682]
14. Desai RM; Koshy ST; Hilderbrand SA; Mooney DJ; Joshi NS, Versatile click alginate hydrogels crosslinked via tetrazine–norbornene chemistry. Biomaterials 2015, 50, 30–37. DOI: 10.1016/j.biomaterials.2015.01.048. [PubMed: 25736493]
15. Koshy ST; Desai RM; Joly P; Li J; Bagrodia RK; Lewin SA; Joshi NS; Mooney DJ, Click-Crosslinked Injectable Gelatin Hydrogels. Adv Healthcare Mater 2016, 5 (5), 541–547. DOI: 10.1002/adhm.201500757.
16. Jivan F; Yegappan R; Pearce H; Carrow JK; McShane M; Gaharwar AK; Alge DL, Sequential Thiol-Ene and Tetrazine Click Reactions for the Polymerization and Functionalization of Hydrogel Microparticles. Biomacromolecules 2016, 17 (11), 3516–3523. DOI: 10.1021/acs.biomac.6b00990. [PubMed: 27656910]
17. Fairbanks BD; Schwartz MP; Halevi AE; Nuttelman CR; Bowman CN; Anseth KS, A versatile synthetic extracellular matrix mimic via thiol-norbornene photopolymerization. Adv Mater 2009, 21 (48), 5005–5010. DOI: 10.1002/adma.200901808. [PubMed: 25377720]

18. Fairbanks BD; Schwartz MP; Bowman CN; Anseth KS, Photoinitiated polymerization of PEG-diacrylate with lithium phenyl-2, 4, 6-trimethylbenzoylphosphinate: polymerization rate and cytocompatibility. Biomaterials 2009, 30 (35), 6702–6707. DOI: 10.1016/j.biomaterials.2009.08.055. [PubMed: 19783300]
19. Grimsley GR; Pace CN, Spectrophotometric determination of protein concentration. Curr Protoc Protein Sci 2003, 33 (1), 3.1. 1–3.1. 9. DOI: 10.1002/471143030.cba03bs15.
20. Culp JS; Hermodson M; Butler LG, The active-site and amino-terminal amino acid sequence of bovine intestinal alkaline phosphatase. Biochimica et Biophysica Acta (BBA)-Protein Structure and Molecular Enzymology 1985, 831 (3), 330–334. DOI: 10.1016/0167-4838(85)90115-3. [PubMed: 3902089]
21. Dangaria SJ; Ito Y; Walker C; Druzinsky R; Luan X; Diekwisch TG, Extracellular matrix-mediated differentiation of periodontal progenitor cells. Differentiation 2009, 78 (2-3), 79–90. DOI:10.1016/j.diff.2009.03.005. [PubMed: 19433344]
22. Hou S; Lake R; Park S; Edwards S; Jones C; Jeong KJ, Injectable Macroporous Hydrogel Formed by Enzymatic Cross-Linking of Gelatin Microgels. ACS Appl Bio Mater 2018, 1 (5), 1430–1439. DOI: 10.1021/acsabm.8b00380.
23. Magin CM; Alge DL; Anseth KS, Bio-inspired 3D microenvironments: a new dimension in tissue engineering. Biomedical Materials 2016, 11 (2), 022001. DOI: 10.1088/1748-6041/11/2/022001. [PubMed: 26942469]
24. Karver MR; Weissleder R; Hilderbrand SA, Synthesis and evaluation of a series of 1, 2, 4, 5-tetrazines for bioorthogonal conjugation. Bioconjugate Chem 2011, 22 (11), 2263–2270. DOI: 10.1021/bc200295y.
25. Jivan F; Fabela N; Davis Z; Alge DL, Orthogonal click reactions enable the synthesis of ECM-mimetic PEG hydrogels without multi-arm precursors. J Mater Chem B 2018, 6 (30), 4929–4936. DOI: 10.1039/C8TB01399C. [PubMed: 30746148]
26. Mikos AG; Herring SW; Ochareon P; Elisseeff J; Lu HH; Kandel R; Schoen FJ; Toner M; Mooney D; Atala A, Engineering complex tissues. Tissue Eng. 2006, 12 (12), 3307–3339. DOI: 10.1089/ten.2006.12.3307. [PubMed: 17518671]
27. Atala A; Kasper FK; Mikos AG, Engineering complex tissues. Sci Transl Med 2012, 4 (160), 160rv12–160rv12. DOI:10.1126/scitranslmed.3004890.
28. Lin NH; Gronthos S; Bartold PM, Stem cells and periodontal regeneration. Aust Dent J 2008, 53 (2), 108–21. DOI: 10.1111/j.1834-7819.2008.000019.x. [PubMed: 18494965]
29. Gottlow J; Nyman S; Karring T; Lindhe J, New attachment formation as the result of controlled tissue regeneration. J Clin Periodontol 1984. DOI:10.1111/j.1600-51x.1984.tb00901.x.
30. Gottlow J; Nyman S; Lindhe J; Karring T; Wennstrom J, New Attachment Formation in the Human Periodontium by Guided Tissue Regeneration - Case-Reports. J Clin Periodontol 1986, 13 (6), 604–616. DOI: 10.111/j.1600-51x.1986.tb00854.x. [PubMed: 3462208]
31. Esposito M; Coulthard P; Thomsen P; Worthington HV, Enamel matrix derivative for periodontal tissue regeneration in treatment of intrabony defects: a Cochrane systematic review. J Dent Educ 2004, 68 (8), 834–44. DOI:10.1002/14651858.cd003875.pub3. [PubMed: 15286106]
32. Sander L; Karring T, Healing of periodontal lesions in monkeys following the guided tissue regeneration procedure. A histological study. J Clin Periodontol 1995, 22 (4), 332–7. DOI: 10.1111/j.1600-051x.1995.tb00156.x. [PubMed: 7622641]
33. Ripamonti U; Hari Reddi A, Tissue Engineering, Morphogenesis, and Regeneration of the Periodontal Tissues By Bone Morphogenetic Proteins. Crit Rev Oral Biol Med 2016, 8 (2), 154–163. DOI:10.1177/10454411970080020401.
34. Rosling B; Nyman S; Lindhe J; Jern B, The healing potential of the periodontal tissues following different techniques of periodontal surgery in plaque-free dentitions: A 2-year clinical study. J Clin Periodontol 1976, 3 (4), 233–250. DOI:10.1111/j.1600-51x.1976.tb00042.x. [PubMed: 1069012]
35. Caton J; Nyman S; Zander H, Histometric evaluation of periodontal surgery. II. Connective tissue attachment levels after four regenerative procedures. J Clin Periodontol 1980, 7 (3), 224–31. DOI: 10.1111/j.1600-51x.1980.tb01965.x. [PubMed: 7000854]

36. Li F; Yu F; Xu X; Li C; Huang D; Zhou X; Ye L; Zheng L, Evaluation of Recombinant Human FGF-2 and PDGF-BB in Periodontal Regeneration: A Systematic Review and Meta-Analysis. Sci Rep 2017, 7 (1), 65. DOI:10.1038/s41598-017-00113-y. [PubMed: 28246406]
37. Han J; Menicanin D; Gronthos S; Bartold PM, Stem cells, tissue engineering and periodontal regeneration. Aust Dent J 2014, 59 Suppl 1, 117–30. DOI:10.1111/adj.12100. [PubMed: 24111843]
38. Pihlstrom BL; Michalowicz BS; Johnson NW, Periodontal diseases. The Lancet 2005, 366 (9499), 1809–1820. DOI:10.1016/S0140-6736(05)67728-8.
39. Giannobile WV; Finkelman RD; Lynch SE Comparison of canine and non-human primate animal models for periodontal regenerative therapy: results following a single administration of PDGF/IGF-I. J Periodontol 1994 65 (12), 1158–1168. DOI:10.1902/jop.1994.65.12.1158. [PubMed: 7877089]
40. Lynch SE; Williams RC; Poison AM; Howell TH; Reddy MS; Zappa UE; Antoniades HN A combination of platelet-derived and insulin-like growth factors enhances periodontal regeneration. J Clin Periodontol 1989 16 (8), 545–548. DOI:10.1111/j.1600-051x.1989.tb02334.x. [PubMed: 2778088]
41. Nevins M; Kao RT; McGuire MK; McClain PK; Hinrichs JE; McAllister BS; Reddy MS; Nevins ML; Genco RJ; Lynch SE; Giannobile WV, Platelet-derived growth factor promotes periodontal regeneration in localized osseous defects: 36-month extension results from a randomized, controlled, double-masked clinical trial. J Periodontol 2013, 84 (4), 456–64. DOI:10.1902/jop.2012.120141. [PubMed: 22612364]
42. Seo B-M; Miura M; Gronthos S; Mark Bartold P; Batouli S; Brahim J; Young M; Gehron Robey P; Wang CY; Shi S, Investigation of multipotent postnatal stem cells from human periodontal ligament. The Lancet 2004, 364 (9429), 149–155. DOI:10.1016/S0140-6736(04)16627-0.
43. Liu HW; Yacobi R; Savion N; Narayanan AS; Pitaru S, A collagenous cementum-derived attachment protein is a marker for progenitors of the mineralized tissue-forming cell lineage of the periodontal ligament. J Bone Miner Res 1997, 12 (10), 1691–1699. DOI: 10.1359/jbmr.1997.12.10.1691. [PubMed: 9333130]
44. Mihaylova Z; Tsikandelova R; Sanimirov P; Gateva N; Mitev V; Ishkitiev N, Role of PDGF-BB in proliferation, differentiation and maintaining stem cell properties of PDL cells in vitro. Arch Oral Biol 2018, 85, 1–9. DOI: 10.1016/j.archoralbio.2017.09.019. [PubMed: 29028628]
45. Ammar MM; Waly GH; Saniour SH; Moussa TA, Growth factor release and enhanced encapsulated periodontal stem cells viability by freeze-dried platelet concentrate loaded thermo-sensitive hydrogel for periodontal regeneration. Saudi Dent J 2018, 30 (4), 355–364. DOI: 10.1016/j.sdentj.2018.06.002. [PubMed: 30202174]
46. Dennison DK; Vallone DR; Pinero GJ; Rittman B; Caffesse RG, Differential effect of TGF-B1 and PDGF on proliferation of periodontal ligament cells and gingival fibroblasts. J Periodontol 1994, 65(7), 641–648. DOI:10.1902/jop.1994.65.7.641. [PubMed: 7608839]
47. Park YJ; Lee YM; Park SN; Sheen SY; Chung CP; Lee SJ, Platelet derived growth factor releasing chitosan sponge for periodontal bone regeneration. Biomaterials 2000, 21 (2), 153–9. DOI: 10.1016/s0142-9612(99)00143-x. [PubMed: 10632397]

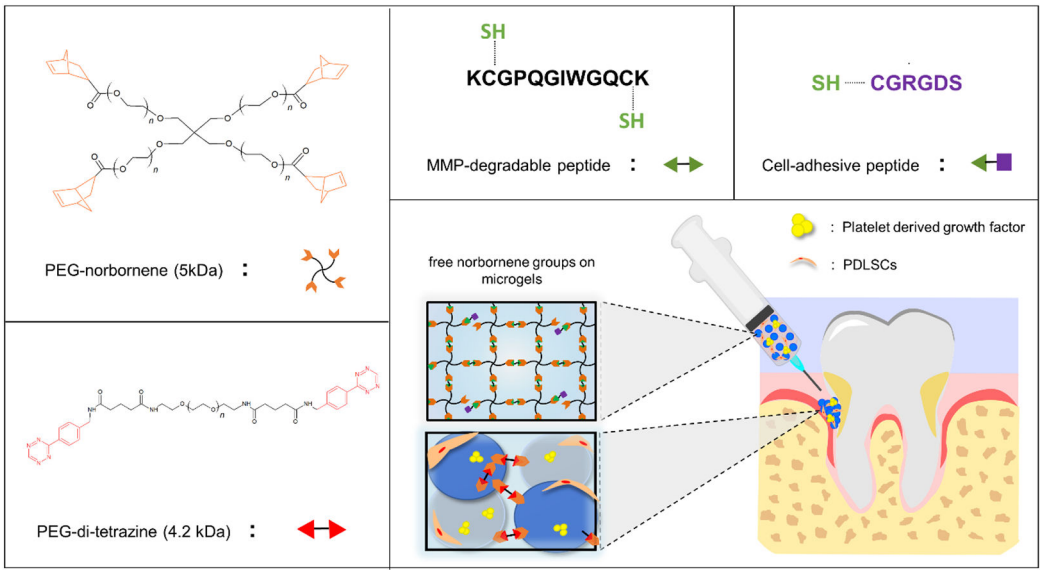

Figure 1.

Overview of materials used to produce PEG microgels and anneal them into TzMAP hydrogels and a schematic illustrating the use of TzMAP hydrogels for delivery of platelet-derived growth factor-BB (PDGF-BB) and periodontal ligament stem cell (PDLSC) into a periodontal defect.

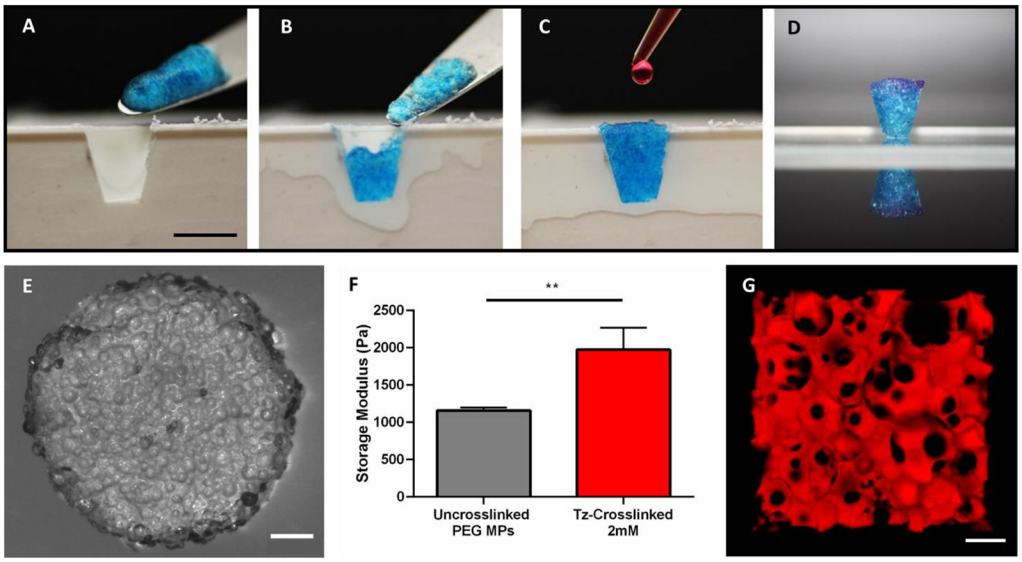

Figure 2.

In situ formation and characterization of TzMAP hydrogels. A-D) Photographs showing formation of a TzMAP hydrogel within a tissue-like defect (scale bar = 5 mm). E) Brightfield stereomicroscopy image of a TzMAP hydrogel (scale bar = 1 mm). F) Storage moduli of microgels before and after annealing (** indicates $p < 0.01$). G) Confocal fluorescence image of a TzMAP hydrogel perfused with tetramethylrhodamine isothiocyanate-labelled dextran to show micropore interconnectivity (scale bar = 200 μm).

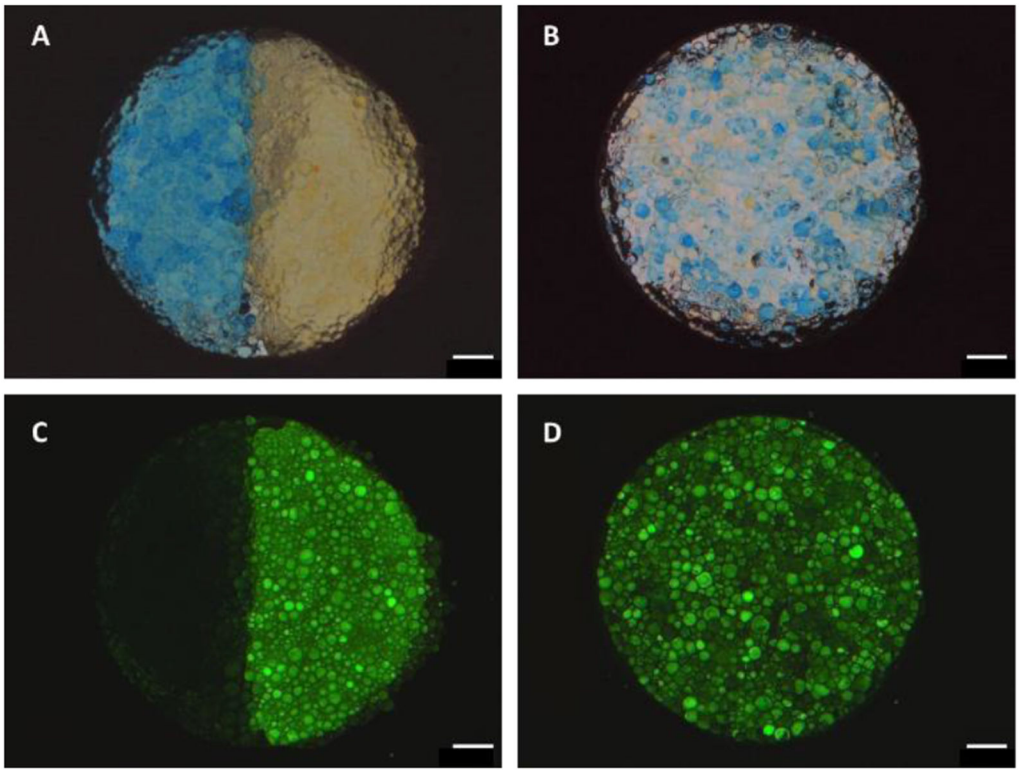

Figure 3.

Heterogeneous TzMAP hydrogels constructed from fluorophore-labelled PEG microgels. Brightfield and fluorescence images of TzMAP hydrogels made from A,C) half Alexa-488/ half Alexa-548 conjugated microgels and B,D) uniformly mixed Alexa-488 and Alexa-548 microgels. Scale bars = 1 mm.

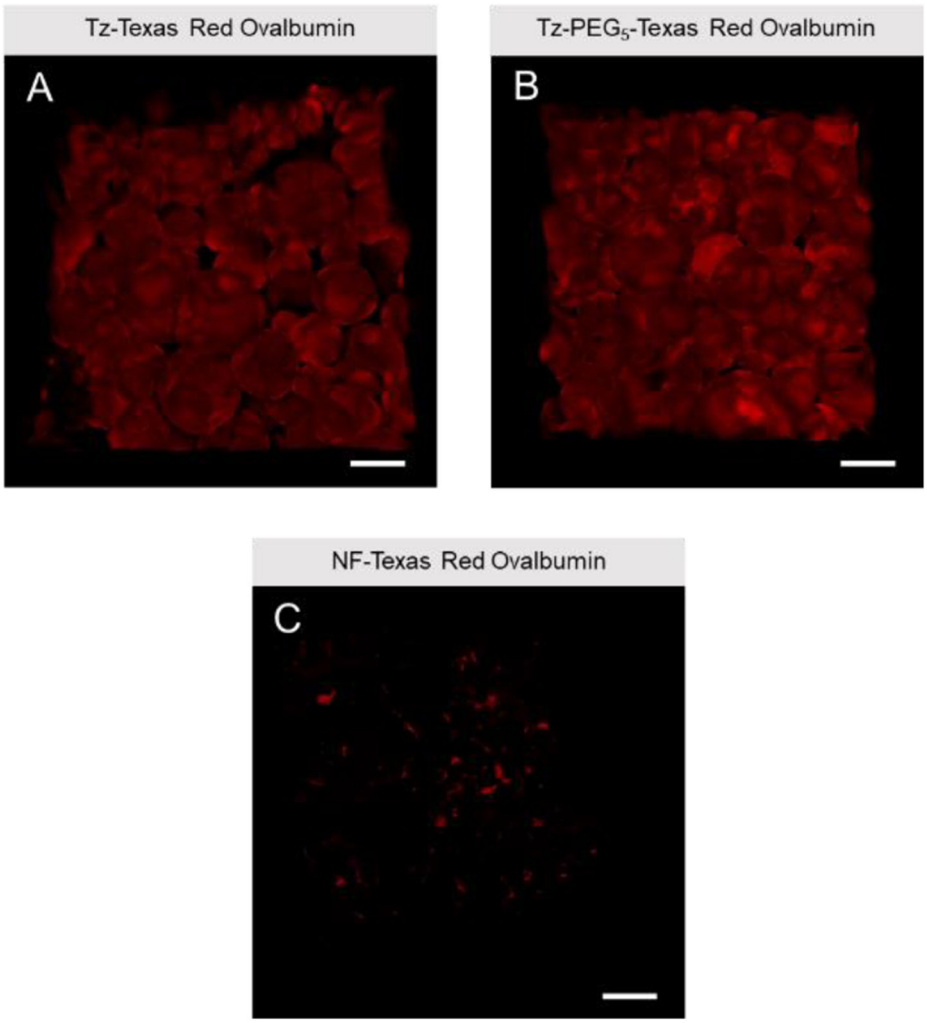

Figure 4.

Confocal fluorescence microscopy images of protein conjugation to TzMAP hydrogels. Texas Red-labelled ovalbumin was modified with A) Tz-NHS or B) Tz-PEG-NHS and incubated with PEG microgels, which were then used to produce TzMAP hydrogels. C) Non-functionalized (NF) Texas Red-labelled ovalbumin was used as a negative control. Scale bars = 200μm.

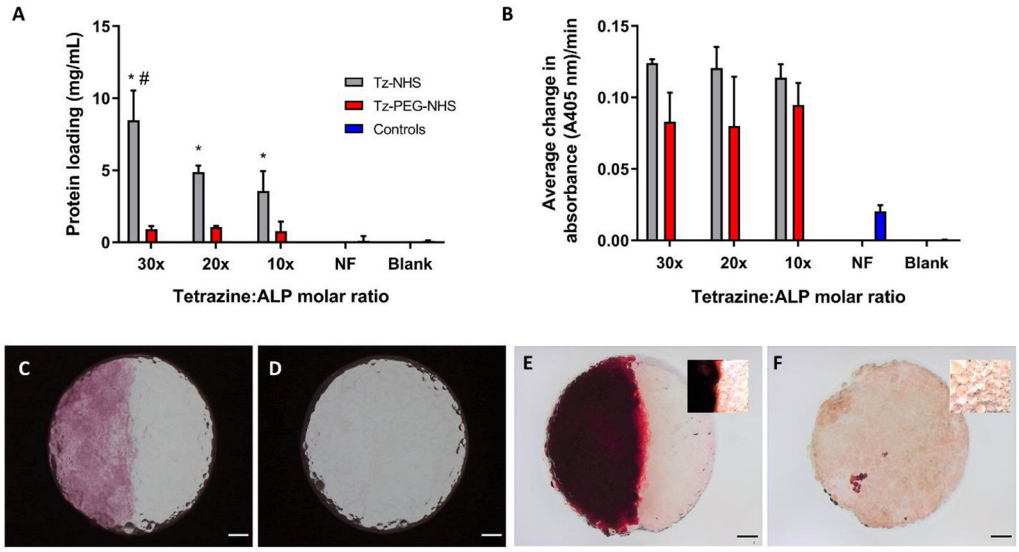

Figure 5.

ALP conjugation and mineralization of TzMAP hydrogels. A) Concentration of ALP conjugated to the microgels using different tetrazine reagents and molar ratios (* indicates $p < 0.05$ for comparisons between Tz-NHS and Tz-PEG-NHS with same equivalents; # indicates $p < 0.05$ for comparisons between 30x equivalents of PEG-NHS to 20x and 10x equivalents of Tz-NHS). B) Microgel bioactivity after ALP conjugation, assessed via the average rate of pNPP conversion. Brightfield images of TzMAP hydrogels produced from C) half ALP-functionalized microgels and half non-functionalized microgels, and D) all non-functionalized microgels. Alizarin red (mineralization) staining after 1-hour incubation with calcium glycerophosphate of E) half ALP-functionalized microgels and half non-functionalized microgels and F) all non-functionalized microgels. Scale bars = 1 mm. Insets show higher magnification images.

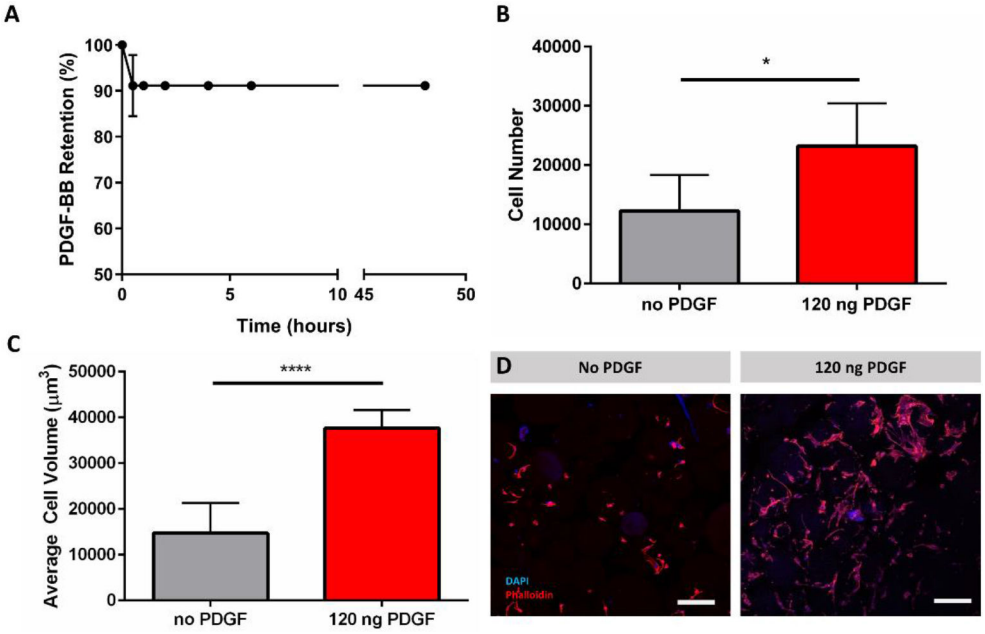

Figure 6.

PDGF-BB loading and PDLSC incorporation within TzMAP hydrogels. A) PDGF-BB retention within TzMAP hydrogels over 48 hours measured indirectly through release of PDGF-BB. B) Number of cells per 50 μL hydrogel observed at 5 days (* indicates $p < 0.05$). C) Average cell volume of PDLSCs at 5 days (**** indicates significant difference; $p < 0.0001$). D) Z-stack projections (200 μm depth) of PDLSCs stained with DAPI (nucleus) and Rhodamine Phalloidin (actin) to visualize cell spreading in TzMAP hydrogels at 5 days (w/ and w/o PDGF-BB). Scale bars = 200 μm.